Strain relaxation and strong impurity incorporation in epitaxial laterally overgrown GaN: Direct imaging of different growth domains by cathodoluminescence microscopy and micro-Raman spectroscopy

F. Bertram,[a] T. Riemann, and J. Christen
Institut für Experimentelle Physik, Otto-von-Guericke Universität, P.O. Box 4120, 39016 Magdeburg, Germany

A. Kaschner, A. Hoffmann, and C. Thomsen
Institut für Festkörperphysik, Technische Universität Berlin, 10623 Berlin, Germany

K. Hiramatsu
Department of Electrical and Electronic Engineering, Mie University, Mie 514-8507, Japan

T. Shibata and N. Sawaki
Department of Electronics, Nagoya University, Nagoya 464-01, Japan

(Received 8 September 1998; accepted for publication 18 November 1998)

Epitaxial lateral overgrowth GaN structures oriented along the $\langle 11\underline{2}0\rangle$ direction were comprehensively characterized by cathodoluminescence (CL) microscopy and micro-Raman spectroscopy. CL microscopy directly visualizes the significant differences between the overgrown areas on top of the SiO_2 mask and the coherently grown regions between the SiO_2 stripes in quantitative correlation with micro-Raman spectroscopy mapping of the local strain and free carrier concentration. The overgrown GaN shows a partial strain relaxation and a high carrier concentration that strongly broadens the luminescence. A strong impurity incorporation is evidenced in the coalescence regions. In contrast, the local luminescence from the areas of coherent (0001) growth is dominated by narrow excitonic emission, demonstrating the superior crystalline quality. © *1999 American Institute of Physics.* [S0003-6951(99)03303-3]

Recently, the use of epitaxial laterally overgrown GaN (ELOG) substrates has been claimed to be responsible for the breakthrough in the lifetime of violet laser diodes.[1] This technique has already been proven effective in reducing dislocation density in GaAs and InP layers on Si substrates[2,3] and has now been successfully applied to GaN.[4–10] However, there is still a lack of understanding of the microscopic mechanisms involved. The defect structure of ELOG films has been widely studied by transmission electron microscopy (TEM), primarily for threading dislocations in GaN films on a sapphire substrate,[11] however, no correlation with the local optical properties has been reported so far. A rough first estimate of the microscopic luminescence was recently given in Ref. 12.

In this letter we present a comprehensive microscopic characterization of near band gap emission by spectrally resolved cathodoluminescence (CL) microscopy and μ-Raman spectroscopy correlating the local optical and electronic properties of the ELO GaN structure.

The sample consists of a 3 μm thick GaN layer grown by metalorganic vapor phase epitaxy (MOVPE) on (0001) sapphire patterned with parallel stripes of 120 nm thick SiO_2 in the $\langle 11\underline{2}0\rangle$ direction. The widths of the windows and the masks are each 10 μm. Selective lateral overgrowth was achieved by 50 μm thick hydride vapor phase epitaxy (HVPE) GaN deposited on the underlying MOVPE GaN layer through the windows in the SiO_2 mask. The low-temperature (5 K) CL measurements were performed in a fully computer-controlled modified scanning electron microscope. In the CL imaging mode the focused electron beam is scanned over the area of interest (256×200 pixels) and *a complete CL spectrum is recorded at each pixel*. The resulting three-dimensional data set $I_{CL}(x, y, \lambda)$ is evaluated *ex situ* to produce local spectra, sets of monochromatic CL images, as well as CL wavelength images (CLWIs) mapping the emission wavelength of the local maximum CL intensity at each sampling point.[13] A spatial resolution of 40 nm can be achieved. The μ-Raman measurements were carried out with spatial resolution of better then 1 μm using a confocal micro optic and the 515.4 nm line of an Ar^+–Kr^+ mixed-gas laser for excitation.

Cross sectional CLWI mapping recorded at an angle of 45° is presented in Fig. 1(b) together with a scanning electron microscope (SEM) image of the ELOG structure [Fig. 1(a)]. Clearly visible are the SiO_2 stripes and the underlying MOVPE buffer layer. The HVPE layer is terminated by sharply defined $\langle 11\underline{2}1\rangle$ facets. The strong variation of the local CL emission wavelength is mapped in the CLWI (the dashed line marks the sample surface). Three different growth regions are clearly visible: the GaN buffer layer at the bottom, the overgrown region above the SiO_2 mask, and the area of coherent growth between the SiO_2 patterns. Areas with no CL intensity are blackened in the CLWIs.

The buffer layer shows a blueshifted (D^0, X) emission at 356.4 nm due to compressive biaxial stress of 0.8 GPa.[14] In the coherent growth region a monochromatic triangle of almost homogeneous emission at 358 nm is visible evolving in the center between the SiO_2 stripes [Fig. 1(b)]. The ELO region is dominated by an inhomogeneous blueshifted emis-

[a]Electronic mail: frank.bertram@physik.uni-magdeburg.de

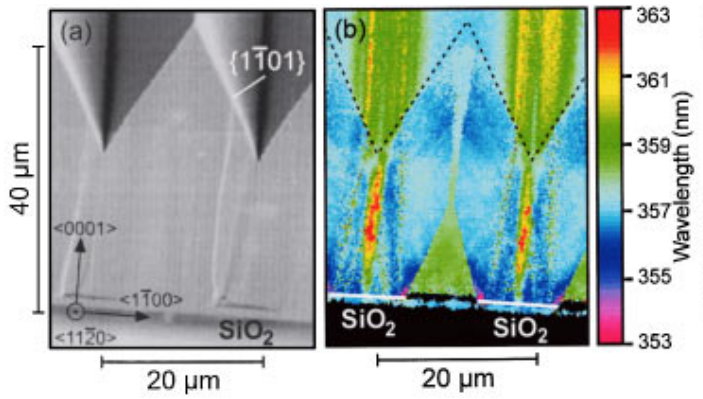

FIG. 1. SEM image (a) and CL wavelength image (b). The two different growth regions indicated in the schematic drawing (c) are clearly visible in the CLWI: the coherently grown area between the SiO_2 stripes and the overgrown area above the SiO_2 stripes (the region of coalescence).

sion around 356 nm showing stripe-like patterns in the *c* direction. Strongly redshifted, the extrinsic CL (362 nm) dominates the ELO coalescence area. At the outer edges of the SiO_2 stripes a strong blueshift ($\lambda < 354$ nm) occurs due to strong local compressive strain.

Figure 2 shows a set of local CL spectra from the overgrown [CLWI=Fig. 2(a) and spectra of Figs. 2(b)–2(g)] and the coherently grown region [CLWI=Fig. 2(h) and spectra of Figs. 2(i)–2(n), respectively]. The CLWI in Fig. 2(a) is a magnified view of the ELO region in Fig. 1(b). The local spectra from this area show broad and blueshifted emissions, as plotted in Fig. 2(d) ($\lambda = 355.9$ nm) and Fig. 2(f) ($\lambda = 357.1$ nm). A strongly redshifted spectrum from the area of coalescence is seen in Fig. 2(c). The broad and blueshifted spectrum from the edges of the SiO_2 stripes is depicted in Fig. 2(e) [$\lambda = 354.1$ nm and full width at half maximum (FWHM)=110 meV]. The CLWI in Fig. 2(h) is a magnified view of the coherently grown region in Fig. 1(b). Starting with the local CL from the buffer [Fig. 2(j)] various points aligned along the ⟨0001⟩ direction crossing over the triangle of the coherently grown region are marked. Spectra from these points clearly show sharp excitonic CL lines: (FX), (D_1^0, X), (D_2^0, X), and (A^0, X) are well resolved [assignment of the transitions in Fig. 2(n) is according to Ref. 15]. With increasing distance to the interface [i.e., scanning from Figs. 2(k)–2(n)] a simultaneous blueshift of 8 meV is observed for all four lines and a high energy shoulder evolves [see Fig. 2(d)] due to electron hole plasma interband recombination. This process, evidencing a large local free carrier concentration, leads to the broad and strongly blueshifted CL emission outside the triangle [see Figs. 2(c)–2(f)]. We would like to point out that no yellow luminescence is observed at any location.

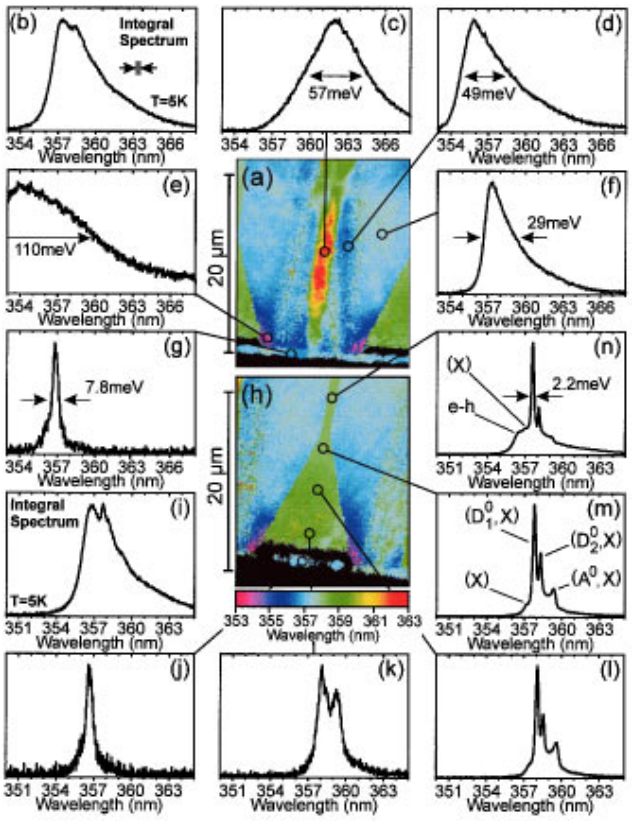

FIG. 2. Local spectra from the overgrown region (c)–(f) dominated by broad CL and the coherently grown region (j)–(n) showing sharp excitonic CL lines (FX), (D_1^0, X), (D_2^0, X), and (A^0, X). The positions of the local spectra are indicated in the CL wavelength images (a) and (h) that are magnified views of the regions of interest: (a) the overgrown area and (h) the region of coalescence. Integral spectra from both regions are depicted in (b) and (i). Spectra from the compressively strained buffer layer are shown in (g) and (j).

In order to understand the spatial dependence of the CL we performed μ-Raman scattering experiments at identical locations. Using the E_2 mode we measure the local strain distribution[16] and the free carrier concentration is determined from the *LPP* modes.[17] Figure 3 shows the results of different μ-Raman line scans over the cross section of the sample. A blue and a red line mark the two different scans in the CLWI [inset of Fig. 3(a)] and in the SEM image [inset of Fig. 3(b)], respectively. The free carrier concentration in the overgrown region jumps to a value of about $9.0 \times 10^{18}\,\mathrm{cm}^{-3}$ above the buffer layer and remains nearly constant up to the surface. *This is evidence of a strong impurity incorporation in the ELO area.* The free carrier concentration in the coherently grown region starts at a level well below our detection limit of about $1.0 \times 10^{18}\,\mathrm{cm}^{-3}$. At 14 μm above the substrate interface a jump occurs to a high concentration of $1.3 \times 10^{19}\,\mathrm{cm}^{-3}$ in perfect agreement with the CLWI that shows this increase of the carrier concentration at the end of the coherently grown region [at the top of the triangle, cf. Fig. 2(h)]. In the coherently grown region we find a lower carrier concentration due to fewer structural defects. In Fig. 3(b) the local distribution of the biaxial stress is depicted. Across the coherently grown region the compressive stress continuously decreases with increasing distance from the substrate from 0.5 GPa in the buffer layer to full

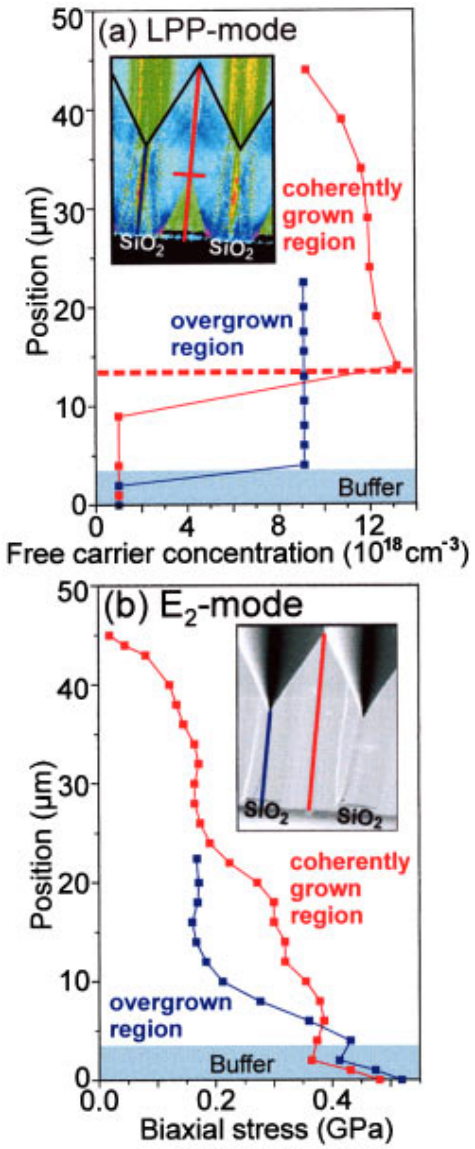

FIG. 3. μ-Raman line scans along the *c* direction as marked in the insets: overgrown region (blue line) and coherently grown region (red line). (a) Free carrier concentration determined from the *LPP* mode and (b) biaxial (compressive) stress calculated from the E_2 Raman mode.

relaxation at the surface. In the ELO region on top of SiO_2 the compressive stress relaxes much faster. However, 10 μm above the SiO_2 the stress relaxation saturates. At the surface we find a residual compressive stress of 0.2 GPa, which fits the value at the same distance from the substrate in the coherently grown region.

In conclusion, ELO GaN structures oriented in the $\langle 11\underline{2}0\rangle$ direction, which results in a strong $\langle 1\underline{1}01\rangle$ faceted surface morphology, were comprehensively micro optically characterized and regions of different growth regimes were identified: The coherently grown regions forming sharply defined triangles in the middle of masks [see the schematic growth model in Fig. 1(c)] show perfect excitonic CL, proving high crystallographic quality, and low free carrier concentration $n<10^{18}\,\mathrm{cm}^{-3}$ evidenced by μ-Raman spectroscopy. In contrast, the ELO regions are of inferior quality, dominated by a blueshifted broad CL emission band and a high carrier concentration $n\gg 10^{18}\,\mathrm{cm}^{-3}$. A strongly redshifted luminescence emerges in the ELO coalescence area due to a high impurity incorporation at the merging crystal planes and resulting voids. At the very edges of the SiO_2 stripes the strongly blueshifted broad luminescence indicates a high impurity incorporation (μ-Raman $n>2\times 10^{19}\,\mathrm{cm}^{-3}$) and a high dislocation density as evidenced by TEM.

[1] S. Nakamura, M. Senoh, S. Nagahama, N. Iwas, T. Yamada, T. Matsushima, H. Kiyoku, Y. Sugimoto, T. Kozaki, H. Umemoto, M. Sano, and K. Chocho, Proceedings of ICNS'97, Tokushima, Japan, edited by K. Hiramatsu (1997), p. 444; J. Cryst. Growth **189/190**, 820 (1998).
[2] D. Pribat, B. Gerad, M. Dupuy, and P. Legagneux, Appl. Phys. Lett. **60**, 2144 (1992).
[3] S. D. Lester, F. A. Ponce, M. G. Craford, and D. A. Steigerwald, Appl. Phys. Lett. **66**, 1249 (1996).
[4] A. Sakai, Appl. Phys. Lett. **71**, 2259 (1997).
[5] D. Kapolnek, S. Keller, R. Ventury, R. D. Underwood, P. Kozodoy, S. P. Den Baars, and U. K. Mishra, Appl. Phys. Lett. **71**, 1204 (1997).
[6] A. Usui, H. Sunakawa, A. Sakai, and A. A. Yamaguchi, Jpn. J. Appl. Phys., Part 1 **36**, 899 (1997).
[7] T. S. Zheleva, O. H. Nam, M. D. Bremser, and R. F. Davis, Appl. Phys. Lett. **71**, 2472 (1997).
[8] D. Kapolnek, X. H. Wu, B. Heying, S. Keller, B. P. Keller, U. K. Mishra, S. P. DenBaars, and J. S. Speck, Appl. Phys. Lett. **67**, 1541 (1995).
[9] S. Nakamura, M. Senoh, S. Nagahama, N. Iwasa, T. Yamada, T. Matsushita, H. Kiyoku, Y. Sugimoto, T. Kozaki, H. Umemoto, M. Sano, and K. Chocho, Appl. Phys. Lett. **72**, 211 (1998).
[10] O.-H. Nam, M. D. Bremser, T. S. Zheleva, and R. F. Davis, Appl. Phys. Lett. **71**, 2638 (1997).
[11] A. Sakai, H. Sunakawa, and A. Usui, Appl. Phys. Lett. **73**, 481 (1998).
[12] J. A. Freitas, O.-H. Nam, R. F. Davis, G. V. Saparin, and S. K. Obyden, Appl. Phys. Lett. **72**, 2990 (1998).
[13] J. Christen, M. Grundmann, and D. Bimberg, J. Vac. Sci. Technol. B **9**, 2358 (1991).
[14] C. Kisielowski, J. Krüger, S. Ruvimov, T. Suski, J. W. Ager, E. Jones, Z. Lilienthal-Weber, M. Rubin, E. R. Weber, M. D. Bremser, and R. F. Davis, Phys. Rev. **54**, 17745 (1996).
[15] H. Siegle, A. Hoffmann, L. Eckey, C. Thomsen, J. Christen, F. Bertram, M. Schmidt, D. Rudloff, and K. Hiramatsu, Appl. Phys. Lett. **71**, 2490 (1997).
[16] C. Kisielowski, J. Krüger, S. Ruvimov, T. Suski, J. W. Ager, E. Jones, Z. Lilienthal-Weber, M. Rubin, E. R. Weber, M. D. Bremser, and R. F. Davis, Phys. Rev. **55**, 4907 (1997).
[17] P. Perlin, J. Camassel, W. Knap, T. Taliercio, J. C. Chervin, T. Suski, I. Grzegory, and S. Porowski, Appl. Phys. Lett. **67**, 2524 (1995).